Eur. Phys. J. Appl. Phys. **88**, 30801 (2019)

https://doi.org/10.1051/epjap/2019190224

THE EUROPEAN PHYSICAL JOURNAL APPLIED PHYSICS

Regular Article

DC radial glow discharge in axial magnetic field at low pressures

Shen Gao[1,*], Jianyuan Feng[2], Wenqi Li[2], and Jihe Cai[2]

[1] School of Electrical and Information, ChangZhou Institute of Technology, ChangZhou 213032, P.R. China
[2] School of Electrical and Electronic Engineering, Shandong University of Technology, ZiBo 255049, P.R. China

Received: 8 August 2019 / Received in final form: 19 October 2019 / Accepted: 16 December 2019

Abstract. The influence of magnetic field on DC radial glow plasma was studied by self-designed coaxial glow discharge device, and the influence of magnetic field on the spatial distribution of plasma density is studied. The experimental results show that the spatial density distribution of plasma from cathode to anode increases gradually in the high-intensity magnetic field, and decreases gradually in the absence of magnetic field. Theoretical analysis of the above results show that the high-intensity magnetic field increases the moving path of the electrons, enhances the collision efficiency between the electrons and the neutral atoms, and makes the discharge plasma density remarkably enhanced.

1 Introduction

DC glow discharge plasma technology is applied widely in many fields, such as plasma etching, plasma material surface treatment, plasma electron beam source, plasma sputtering spraying and so on [1–3]. Many scholars have done a lot of research on the theory of the glow discharge. Most of the literatures are plate electrode structure [4–8]. Other documents are hollow cathode or abnormal glow discharge in crossed electric and magnetic fields [9–12]. In the above structure, the electric field and magnetic field are not symmetrical and the electric field distribution is not uniform [13], which makes the establishment of mathematical model more complicated.

This paper established a device of the structure of magnetron. In this model, the electric and magnetic fields are uniform and symmetrical, the electric field is perpendicular to the magnetic field. The spatial distribution of plasma density under different magnetic field conditions was measured. For better understanding of physical processes in various types of gas discharge numerical models are often applied. In this work, the fluid simulation on radial glow discharge model in axial magnetic field at low pressure is performed. Based on the analysis of the simulation results, the influence of magnetic field on the glow discharge plasma is obtained. The conclusions obtained by theoretical analysis are in agreement with the experimental results.

2 Experimental apparatus and results

The structure of magnetron glow discharge is shown in Figure 1. The distance between cathode and anode is 16 mm. The cathode is solid cylinder structure and the anode is hollow cylinder. The cylindrical height of cathode and anode is 25 mm. The inner diameter of the magnet is 20 mm and the outer diameter is 40 mm. During the experiment, the magnetic field intensity at the axial is changed by adjusting the relative position of the magnet or increasing the number of magnets. The distribution of electric and magnetic fields in glow discharge of magnetron is shown in Figure 2. The magnetic field is generated by upper and lower magnets and distributed in the gap between electrodes. The distribution of steady magnetic field in the discharge space is the axial direction. The electric field is produced by the voltage at both ends of the anode and cathode and the direction of electric field distribution is radial.

The relationship between magnetic field and glow discharge pressure is shown in Figure 3. The ignition pressure of coaxial glow discharge is 1.3 pa without applied magnetic field. With the increase of magnetic field, the glow pressure decreases gradually. When the magnetic field is 25.8 mT, the ignition pressure decreases to 0.04 pa.

In the experiment, the plasma density was measured by double probe method. In order to avoid the influence of magnetic field on the measurement results of plasma density, the relative positions of the two probes in the experiment are parallel to the magnetic lines of flux. Figure 4 shows the spatial distribution of plasma density under different magnetic fields. Under high-intensity magnetic field, the plasma density increases from cathode to anode, and decreases gradually from cathode to anode in the absence of magnetic field. Figure 5 is an experimental phenomenon of glow discharge in high-intensity magnetic field, and Figure 6 is an experimental phenomenon of glow discharge in a weak magnetic field. It can be seen from Figure 6 that the glow discharge near the cathode is brighter than that at the anode.

* e-mail: gs595198290126.com

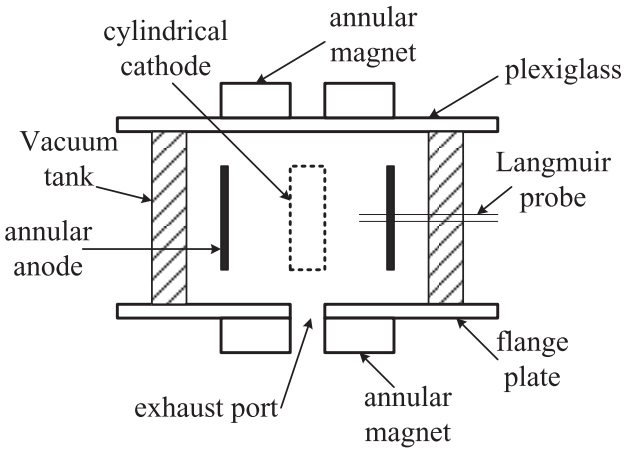

Fig. 1. Magnetron glow discharge device.

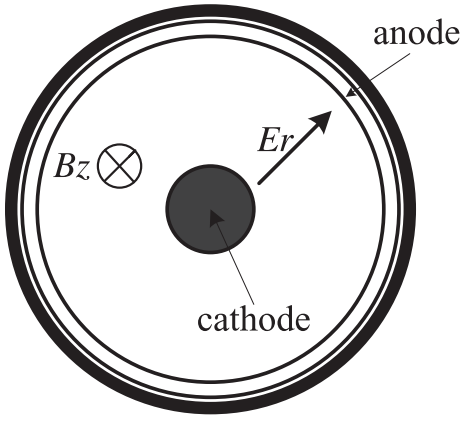

Fig. 2. Radial glow discharge in axial magnetic field.

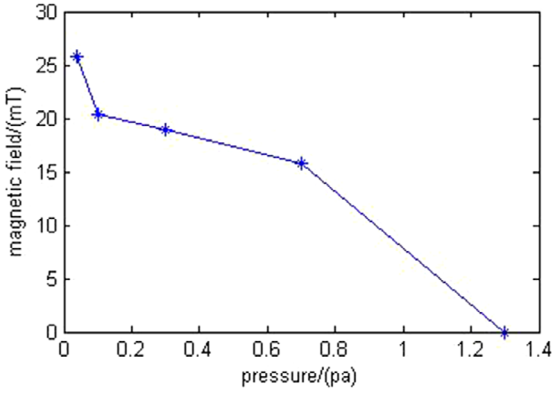

Fig. 3. The relationship between ignition pressure and magnetic field.

3 Theoretical analysis

According to Figure 2, the physical model is based on the following assumptions:

– The direction of the applied magnetic field is perpendicular to the direction of the electric field. Edge effect of electric field is neglected.

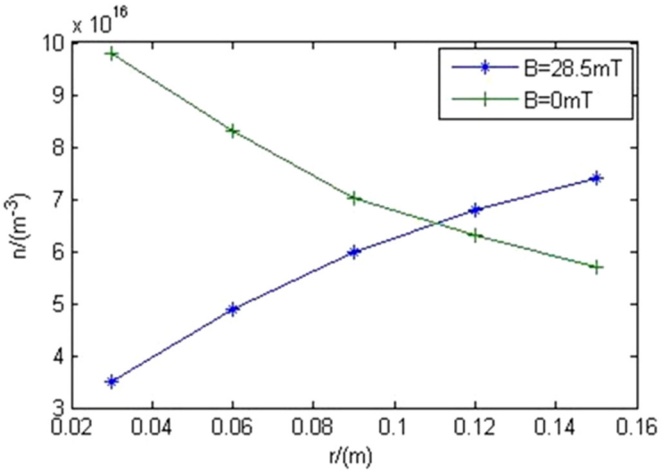

Fig. 4. Plasma density distribution under different magnetic fields.

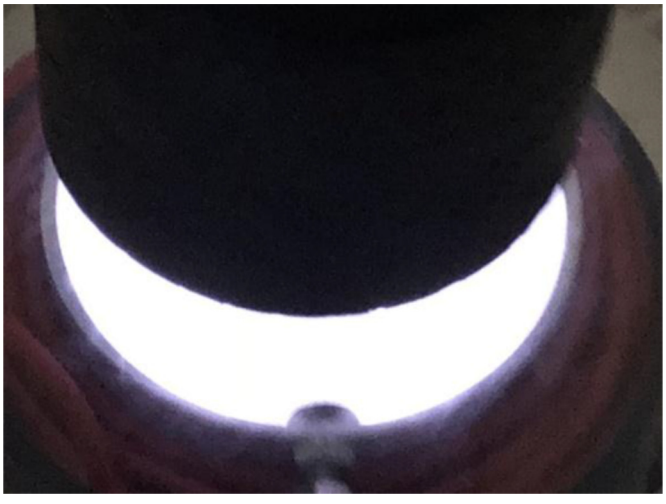

Fig. 5. Glow discharge under high-intensity magnetic field.

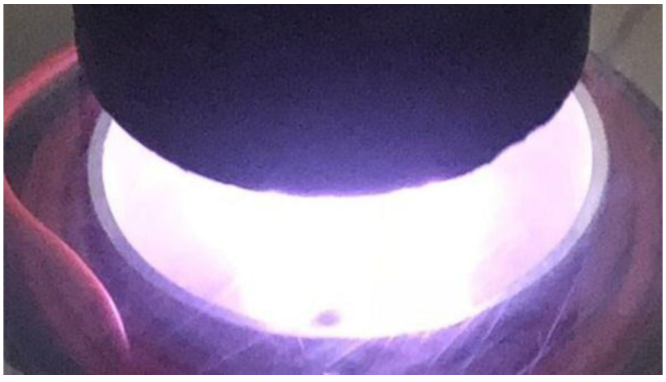

Fig. 6. Glow discharge under weak magnetic field.

– Plasma formation is mainly a result of electrons collision with neutral atoms, while generation of negative ions and other factors are not considered.
– It is generally considered that in low-temperature glow discharge plasma model, ions maintain the same temperature as neutral gas. Hence, there is no need to consider energy equation [14,15].

The basic equations employed in this theoretical formulation are the particle and momentum conservation equations coupled with one of the Maxwell equations:

$$\frac{\partial n_\alpha}{\partial t} + \nabla\cdot(n_\alpha \mathbf{u}_\alpha) = \xi_i n_e \tag{1}$$

$$m_\alpha n_\alpha \left\{\frac{\partial}{\partial t} + \mathbf{u}_\alpha\cdot\nabla\right\}\mathbf{u}_\alpha = q_\alpha n_\alpha(\mathbf{E} + u_\alpha \times \mathbf{B}) - \nabla(kT_\alpha n_\alpha) - m_\alpha \mathbf{u}_\alpha n_\alpha \nu_{\alpha n} \tag{2}$$

$$\nabla\cdot\mathbf{E} = \frac{e}{\varepsilon_0}\sum_{\alpha=i,e} n_\alpha. \tag{3}$$

In the above equations the various notations are defined as follows: ξ_i is the ionization frequency; subscript α represent electron or ion; n_α, $\mathbf{u}_\alpha$, m_α and T_α are, respectively, the number density, average velocity, mass, and temperature; $\nu_{\alpha n}$ is the respective collision frequency of electrons and positive ions with neutral particles and they are assumed to be constants in this case; $\mathbf{E}$ is the electric field; $\mathbf{B}$ is the magnetic field; q_α is the electronic charge and ε_0 is the permittivity constant; k is the Boltzmann constant.

We shall first consider these equations for a steady state case in which all the terms involving time derivative vanish. Next, we neglect the inertial terms $\{\mathbf{u}_\alpha\cdot\nabla\}\mathbf{u}_\alpha$ in equation (2), as in the present case the average flow velocity in general is much smaller than the average speed of the random thermal motions 14. Equation (2) becomes the following form

$$q_\alpha\mathbf{E} + q_\alpha(\mathbf{u}_\alpha \times \mathbf{B}) - \frac{kT_\alpha}{n_\alpha}\nabla n_\alpha = m_\alpha \nu_{\alpha n}\mathbf{u}_\alpha. \tag{4}$$

According to the model assumptions (1), electric field is axial component, $E_\theta = E_z = 0$ and $B_\theta = B_r = 0$. Taking into account (3), conditions assumed by the model, component form of the equation (4) parallel to magnetic field is:

$$\mathbf{u}_{\alpha\|} = -D_{a\|}\frac{\nabla n_\alpha}{n_\alpha} \tag{5}$$

where

$$D_{a\|} = \frac{kT_\alpha}{m_\alpha \nu_{\alpha n}}. \tag{6}$$

In the direction perpendicular to the magnetic field, the equation (4) is

$$\mathbf{u}_\alpha = b_{a\perp}\mathbf{E} + b_{ad}\mathbf{E}\times\mathbf{b}_0 - D_{ad}\nabla n_\alpha \times \mathbf{b}_0 - D_{a\perp}\frac{\nabla_\perp n_\alpha}{n_\alpha} \tag{7}$$

where

$$\omega_{an} = \frac{q_a\mathbf{B}}{m_a} \tag{8}$$

$$\mathbf{b}_0 = \frac{\mathbf{B}}{B_0} \tag{9}$$

$$b_{a\perp} = \frac{q_\alpha \nu_{\alpha n}}{m_\alpha(\nu_{an}^2 + \omega_{an}^2)} \tag{10}$$

$$b_{ad} = \frac{1}{B_0(1 + \nu_{an}^2/\omega_{an}^2)} \tag{11}$$

$$D_{ad} = \frac{kT_\alpha}{q_\alpha n_\alpha B_0(1 + \nu_{\alpha n^2}/\omega_{an}^2)} \tag{12}$$

$$D_{a\perp} = \frac{kT_\alpha \nu_{\alpha n}}{m_\alpha(\nu_{\alpha n^2} + \omega_{an}^2)}. \tag{13}$$

Diffusion coefficient and mobility satisfy Einstein relation:

$$\frac{b_{a\perp}}{D_{a\perp}} = \frac{q_\alpha}{kT_\alpha}. \tag{14}$$

The plasma is assumed to be uniformly distributed in the angular and axial direction, we obtained

$$\nabla\cdot(\mathbf{u}_\alpha n_\alpha) = b_{a\perp}\frac{En_\alpha}{r} + b_{a\perp}E\frac{\partial n_\alpha}{\partial r} + b_{a\perp}n_\alpha\frac{\partial E}{\partial r} - \frac{D_{a\perp}}{r}\frac{\partial n_\alpha}{\partial r} - D_{a\perp}\frac{\partial^2 n_\alpha}{\partial r^2}. \tag{15}$$

Ionization frequency can be expressed as follows

$$\zeta_i = \beta_1 \mathbf{u}_E \tag{16}$$

where

$$\beta_1 = Ap\,\exp\left(-\frac{B_c p}{\mathbf{E}}\right). \tag{17}$$

In the above equations, $\mathbf{u}_E$ is the electron drift velocity along the radial direction. β_1 is the Townsend ionization coefficient and is a function of the gas pressure p and electric field $\mathbf{E}$. A and B_c are constants.

Equations (1), (3), (7), (15), (16) constitute final form of glow discharge plasma physics model equation under axial magnetic field condition. In the above equations, except n_e, n_i, $\mathbf{E}$, all other parameters can be regarded as constants in calculation.

In order to solve the above differential equations, the appropriate boundary conditions should be selected. Boundary condition for electric potential at the cathode is $\varphi = 0$ and at the anode $\varphi = V_0$ is equal to the applied voltage. The value of electron number densities at the anode is $\frac{\partial n_e}{\partial r} = 0$ and at the cathode $n_e = n_0$; the value of ion

number densities at the anode is $n_i = 0$ and at the cathode $\frac{\partial n_i}{\partial r} = 0$. In the absence of a magnetic field, the mobility of electrons and ions is expressed as

$$b_e = \frac{4.2 \times 10^5}{p\frac{293}{T}} \tag{18}$$

$$b_i = \frac{2280}{p\frac{293}{T}}. \tag{19}$$

Using (18) and (19), the collision frequency of electron and positive ion can be expressed as

$$\nu_{en} = \frac{e}{m_e} p \frac{293}{T} \frac{1}{4.2 \times 10^5} \tag{20}$$

$$\nu_{in} = \frac{e}{m_i} p \frac{293}{T} \frac{1}{2280}. \tag{21}$$

Numerical modeling based on one dimensional extended fluid model was carried out for the voltage 600 V, the pressure range 0.01 Pa–0.1 Pa and the cathode rod radius 1 mm, anode cylinder radius is 40 mm. The physical process detailed analysis for high-intensity magnetic field of 20 mT, and low-intensity magnetic field of 0 mT–0.0002 mT will be presented.

The number density profiles of electrons and ions of glow discharge at 20 mT magnetic field are shown in Figure 7. In the case of low air pressure, the electron density and ion density distribution show increasing trend. This is the same as the experimental results under the condition of 25.8 mT magnetic field in Figure 4. At the cathode, the ion density increases gradually as a result of collision ionization. Figure 8 shows the distribution of the electric field. The electric field is almost constant in the range of 0.02–0.04 m. The electric field increases gradually near the cathode. The distribution trend of electric field is consistent with that of normal glow discharge. In a flat glow discharge without magnetic field, the ion density in the cathode region is larger than the electron density, which is due to the fact that the electron diffusion rate is much higher than the ion diffusion rate.

$$D_i \ll D_e. \tag{22}$$

In the magnetron model, the diffusion rate of electrons is much lower than that of ions due to the influence of magnetic field, which makes the density of electrons in the cathode region larger than that of ions. According to the equation (13)

$$D_i \gg D_e. \tag{23}$$

Figures 9–11 are the spatial distribution of electron density, ion density and electric field at different pressures in 20 mT magnetic field. With the increasing of the pressure, the electron density, ion density and electric field increased firstly and then decreased trend in the whole discharge interval.

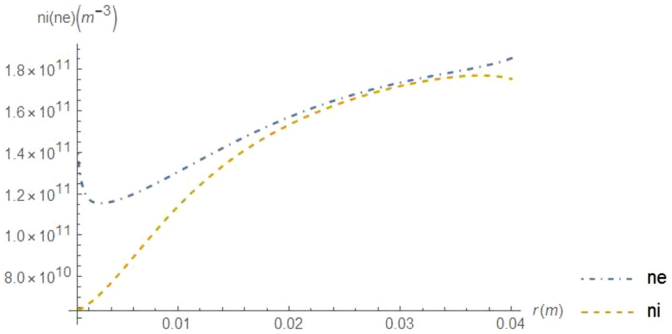

Fig. 7. Electron density and ion density distribution in 20 mT magnetic field.

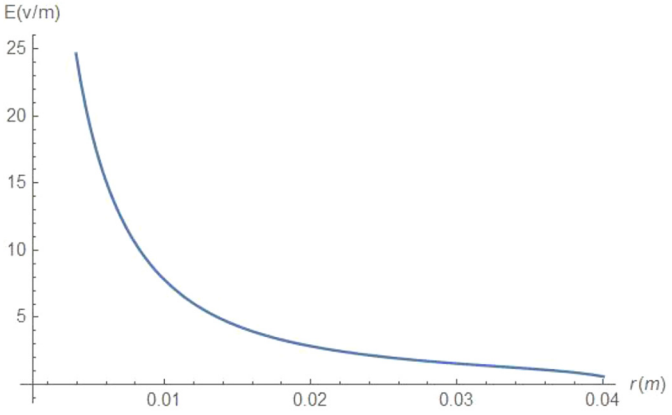

Fig. 8. Electric field distribution in 2 mT magnetic field.

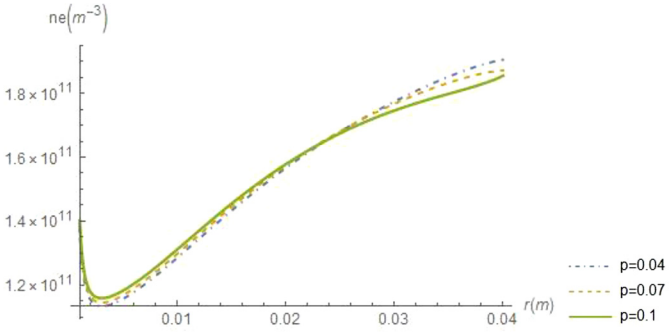

Fig. 9. Electron density distribution at different pressures.

Figure 12 shows the electron density distribution at different weak magnetic fields. Under the condition of low-intensity magnetic field, the electron density increases with the increase of magnetic field intensity and the spatial distribution of electron density decreases gradually, which is consistent with the trend that the radial distribution of electron density is Bessel function in the absence of magnetic field.

In the discharge process, electrons are constrained by electric and magnetic fields. The equations of motion of electrons are as follows

$$m_e \frac{d\vec{v}}{dt} = -e(-\vec{E} + \vec{v} \times \vec{B}). \tag{24}$$

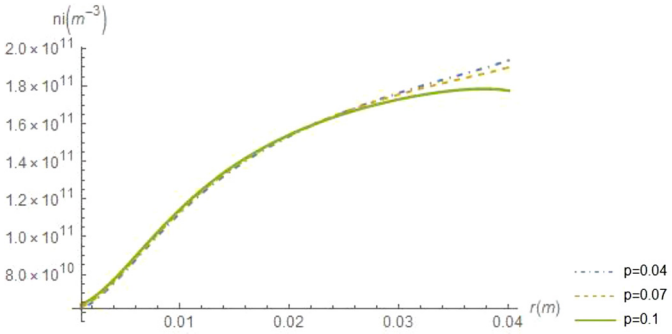

Fig. 10. Ion density distribution at different pressures.

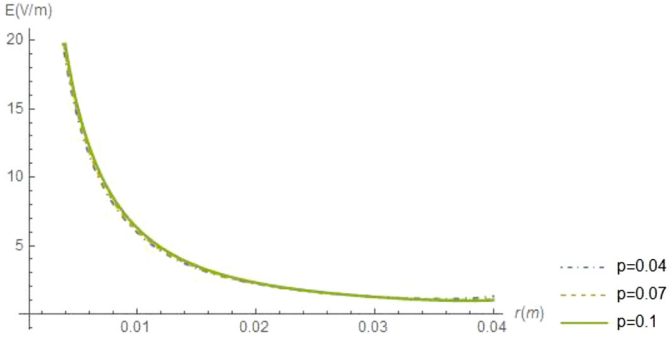

Fig. 11. Electric field distribution at different pressures.

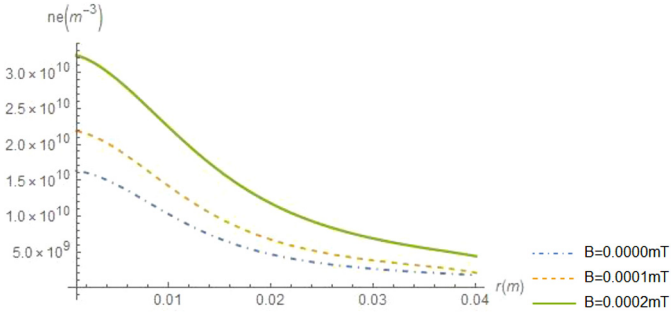

Fig. 12. Electron density distribution at different magnetic field.

Based on the analysis of the electric field and magnetic field of Figure 1, equation (24) is expanded to scalar expression on each axis as follows.

$$\begin{cases} m_e \dfrac{d\vec{v}_r}{dt} = eE_r - e\vec{v}_\theta B_z \\ m_e \dfrac{d\vec{v}_\theta}{dt} = e\vec{v}_r B_z. \end{cases} \tag{25}$$

The initial condition of electron motion as follows

$$t = 0, \vec{v}_r = 0, \vec{v}_\theta = 0, \vec{v}_z = 0. \tag{26}$$

$$t = 0, r = 0, \theta = 0, z = 0. \tag{27}$$

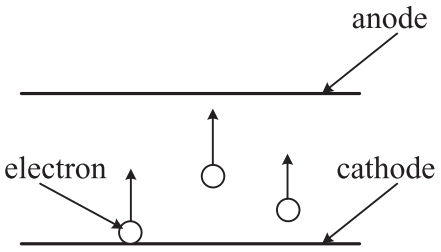

Fig. 13. Electron trajectories in the absence of magnetic field.

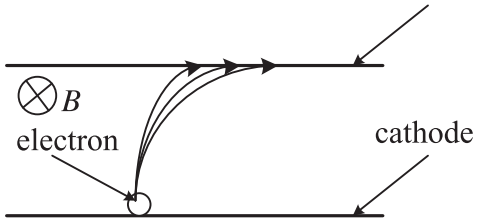

Fig. 14. Electron trajectories in the weak magnetic field.

Combined equations (25), (26) and (27), we obtain electronic equation of motion

$$\begin{cases} r = -\dfrac{a_r}{\omega_z^2}\cos\omega_z t + \dfrac{a_r}{\omega_z^2} \\ \theta = \omega_z t \end{cases} \tag{28}$$

where

$$a_r = eE/m_e, \omega_z = eB/m_e. \tag{29}$$

The electron trajectory is from cathode to anode in magnetic field 0 mT (Fig. 13). When the magnetic field is very weak, the electron cannot form a complete cyclotron motion between the cathode and anode, as shown in Figure 14. For example, when the magnetic field of the electron is 0.0002 mT and the voltage is 500 V, the gyration radius of the electron is about 2 m, which is much larger than the distance between the anode and the cathode. According to the equation (28), under the condition of weak magnetic field, electrons have larger trajectories and the magnetic field increases the path of motion of electrons and increases the collision probability between electrons and neutral atoms, as shown in Figure 14. In this case (weak magnetic field), the density of electrons increases with the increase of magnetic field due to the increase of collision probability of electrons and neutral atoms, but the spatial density distribution of electrons is the same as that without magnetic field, as shown in Figure 12. This is because the electron does not perform complete electron cyclotron all the time, the electron can't make the plasma density accumulate in the process of ionization, and the introduction of magnetic field only increases the motion path of the electron.

Under high-intensity magnetic field, the initial electrons can only move on the cathode surface and produce a thin plasma layer on the plasma positive column region. With the first thin plasma as the substrate, electrons in the

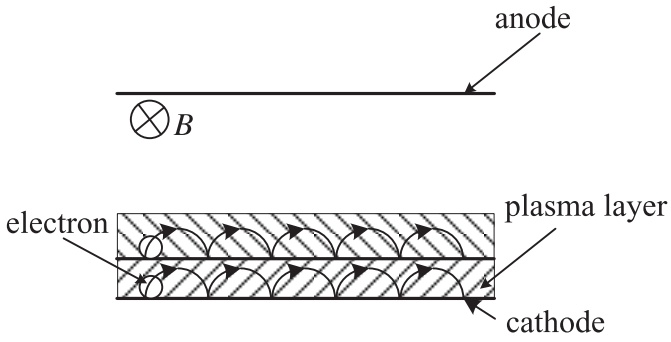

Fig. 15. Electron trajectories in high-intensity magnetic field.

plasma layer collide with neutral atoms to produce another thin plasma in the high-intensity magnetic field, as shown in Figure 15. Due to impact ionization, the electron density in the plasma is larger than the initial electron density. Therefore, in the subsequent process of ionization, the increase of electron density makes the ionization stronger. Therefore, the density of the next thin plasma is higher than that of the previous one. The plasma layer is continuously produced and superimposed, and eventually develops to the anode. The plasma density in the whole space is increasing.

4 Conclusions

In the experiment of magnetron glow discharge, the magnetic field can reduce the glow pressure of glow discharge. At the same time, the plasma density increases gradually from cathode to anode in high-intensity magnetic field. In the absence of magnetic field, the plasma density decreases gradually from cathode to anode. 1D fluid model was built for describing magnetron model at low pressure. In this work, we investigated the effect of magnetic field on the characteristic of this type of discharge. The results show the high-intensity magnetic field increases the moving path of the electrons, enhances the collision efficiency between the electrons and the neutral atoms, and makes the discharge plasma density remarkably enhanced.

This work is supported by the Natural Science Foundation of the Jiangsu Higher Education Institutions of China (19KJB140006), Changzhou Science and Technology Program of China (CJ20179061), and Changzhou Science and Technology Program of China (CJ20189024).

References

1. Y.N. Wang, Y. Liu, S. Zhang, G.Q. Lin, J. Plasma Phys. **78**, 673 (2012)
2. A. Krauze, J. Virbulis, A. Kravtsov, Mater. Sci. Eng. **355**, 012008 (2018)
3. X.L. Zhao, S.X. Chen, K. Chen, B.K. Chen, Plasma Sci. Technol. **16**, 21 (2014)
4. S. Surzhikov, J. Shang. Plasma Sources Sci. Technol. **23**, 054017 (2014)
5. M.N. Stankov, M.D. Petkovic, V.LJ. Markovic, S.N. Stamenkovic, Plasma Phys. **59**, 328 (2013)
6. A.S. Petrusev, S.T. Surzhikov, Plasma Phys. Rep. **34**, 239 (2007)
7. M. Hu, S.D. Wan, L. Zhong, H. Liu, H. Wang, Acta Phys. Sin. **61**, 045201 (2012)
8. L. Pekker, Plasma Sources Sci. Technol. **4**, 31 (1995)
9. A.V. Isakov, V.P. Kolesnik, A.M. Okhrimovskyy, N.P. Stepanushkin, A.A. Taran, Probl. At. Sci. Technol. **20**, 171 (2014)
10. Y.Y. Fu, H.Y. Luo, X.B. Zhou, X.X. Wang, Plasma Sources Sci. Technol. **23**, 065035 (2014)
11. O. Baranov, M. Romanov, S. Kumar, X.X. Zong, K. Ostrikov, J. Appl. Phys. **109**, 063304 (2011)
12. E.S. Dzlieva, L.G. Dyachkov, L.A. Novikov, S.I. Pavlov, V. Yu. Karasev, Europhys. Lett. **123**, 15001 (2018)
13. S.T. Surzhikov, J.S. Shang, J. Comput. Phys. **199**, 437 (2004)
14. S.T. Pai, X.M. Guo, T.D. Zhou, Phys. Plasmas. **3**, 3842 (1996)
15. S.T. Pai, J. Appl. Phys. **71**, 5820 (1992)

Cite this article as: Shen Gao, Jianyuan Feng, Wenqi Li, Jihe Cai, DC radial glow discharge in axial magnetic field at low pressures, Eur. Phys. J. Appl. Phys. **88**, 30801 (2019)